Highlights of Spanish Astrophysics VIII, Proceedings of the XI Scientific Meeting of the Spanish Astronomical Society held on September 8–12, 2014, in Teruel, Spain. A. J. Cenarro, F. Figueras, C. Hernández-Monteagudo, J. Trujillo Bueno, and L. Valdivielso (eds.)

PEP/HerMES/COSMOS: What are the dust properties of z ∼ 3 lyman break galaxies?

Javier Álvarez-Márquez[1], Denis Burgarella[1], Veronique Buat[1], Sebastien Heinis[2], and the PEP/HerMES/COSMOS teams

[1] Aix-Marseille Université, CNRS, LAM (Laboratoire d'Astrophysique de Marseille), UMR7326, 13388, France (email: javier.alvarez@lam.fr)
[2] University of Maryland, Dept. of Astronomy, College park, MD

Abstract

Aims. We explore the dust properties in a statistical way of a sample of Lyman break galaxies (LBGs) that can not be individually detected in Herschel maps.
Methods. We apply a stacking method in the Herschel and AzTEC maps to LBGs selected at $2.5 < z < 3.5$ by dropout technique. Thanks to the size of the sample (∼22 000 LBGs), we can split it in several bins as a function of their ultraviolet luminosity ($L_{\rm FUV}$), their ultraviolet slope ($\beta_{\rm UV}$) and their stellar mass (M_*) to better catch their variety. The stacking is corrected for the incompleteness in the priors and for the clustering of the stacked galaxies in ultraviolet.
Results. We obtain the full infrared spectral energy distributions of our LBGs as a function of their $L_{\rm FUV}$, their $\beta_{\rm UV}$ and their M_* and we can characterize them in terms of their dust attenuation $A_{\rm FUV}$, their star formation rate (SFR).

1 Introduction

Lyman Break Galaxies (LBGs) are currently the largest population of star-forming galaxies known to be at high redshift, $z > 2.5$. This is due to the efficiency of the selection of LBGs in broad band colors [25]. However, the dust properties of these LBGs are still badly known due to their faintness in the far infrared (FIR) and sub-millimeter (submm) wavelength range, which is very likely related to the low dust content.

Most if not all of the cosmological information we have been able to gather on the Cosmic star formation history and dustiness have been extracted from LBGs at $z > 3$. However, only at $z < 2$ do we have a statistical and representative information on the dust

properties. [5] showed that, even at $z = 3.6$ about half of the star formation still resides in the FIR. This means that neglecting what happens in the FIR could lead to uncertainties in the estimated star formation rates (SFRs) and finally in our knowledge of the formation and evolution of the galaxies. Beyond that, we are interested in learning what are the dust properties of the LBGs at $z \sim 3$ and higher redshift in the future, to better physically understand them.

2 Data and sample

We base this study on data from the COSMOS survey, which gathered deep multi-wavelength observations from X-ray to radio covering 2 deg^2 We use optical data (images: [6], photometry: [16], Far-infrared data from PACS (PEP, [13]) and SPIRE (HerMES, [19]) bands and AzTEC (1.1 mm) data [1].

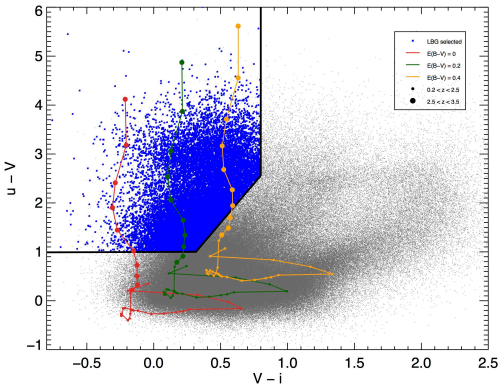

Figure 1: LBGs selection in a color-color diagram. The gray dots are the full sample from COSMOS field, the blue dots are the LBGs selected at $2.5 < z < 3.5$. The tracks are the star-forming galaxies simulated ($0.2 < z < 3.5$).The limits have beed defined by using the code CIGALE to model galaxies (see text).

Our LBGs at $z \sim 3$ are selected by employing the classical dropout technique with the broad-band filters u, V and i (e.g. [25]). We create synthetics spectra and SEDs with CIGALE code (python v0.4, [5] and [17])[1] to compute selection criterion (Eq. 1) according to our broad-band filters. We simulate star-forming galaxies with constant star formation history (SFH), stellar population of 100 Myr old, subsolar metallicity ($0.2\,Z_{\odot}$) and three different values for the V-band attenuation ($E(B-V) = 0, 0.2, 0.4$). Figure 1 shows the expected color in redshift evolution ($0.2 \leq z \leq 3.5$) for the synthetic star-forming galaxies, therefore we derive the analytical selection criterion for the object detected in the three band images:

[1] http://cigale.lam.fr/

$$\begin{aligned} u - V_J &> 1 \\ V_J - i^+ &< 0.8 \\ u - V_J &> 3.2(V_J - i^+) \end{aligned} \tag{1}$$

The catalogue from [16] is based on i-band detection down to $0.6\,\sigma$ above the background. In addition to the selection criterium, we only select the objects with $log(L_{\rm FUV}[{\rm L}_\odot]) > 10.2$ corresponding to the 50 % of completeness for objects detected in V and i bands. In order to clean the sample from lower-redshift interlopers, we only select those galaxies whose photometric redshifts are within $2.5 \leq z \leq 3.5$. The final sample contains ∼22 000 LBGs with a mean redshift, $\langle z \rangle = 2.98 \pm 0.25$. The large sample allows us to split it in different bins as a function of $L_{\rm FUV}$, $\beta_{\rm UV}$ and $\rm M_*$ to better catch their variety.

3 Stacking method and results

Only a few LBGs have been directly detected in the PACS (e.g. [20]), IRAC and MIPS (e.g. [14]) maps at $z \sim 3$. Less than 0.5 % of our sample is detected in the SPIRE band, therefore, we focus on statistical (stacking) analysis of these LBGs to study their dust properties.

The stacking is a technique that combines the signal of multiple sources, which have been selected previously in other wavelength observations [10]. We use the IAS library ([2] and [3]) to perform the stacking in PACS (100 μm and 160 μm images), SPIRE (250 μm, 350 μm and 500 μm images) and AzTEC (1.1 mm image). We apply a correction for the incompleteness in the priors and for the clustering of the stacked galaxies.

The total IR luminosity ($\rm L_{IR}$) is estimated by integrating over the range $8 < \lambda < 1000\,\mu$m the best fit to the [9] templates, obtained with the SED-fitting code CIGALE (Fig. 2).

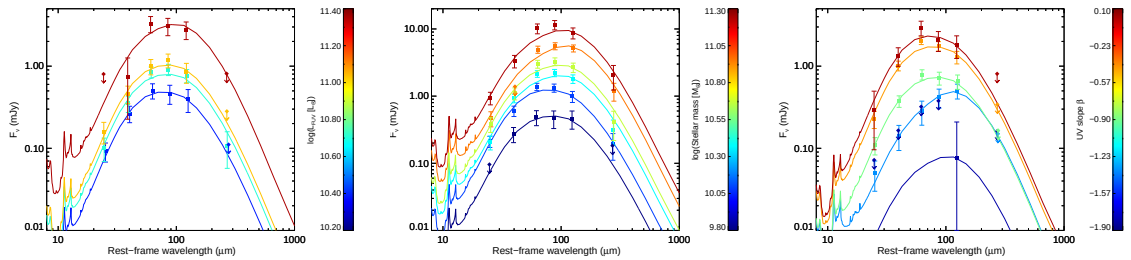

Figure 2: SEDs and best models fit of our stacked LBGs as a function of $L_{\rm FUV}$ (left), stellar mass (center) and UV slope (right) using [9] templates inside CIGALE. The square points are the measurements on stacked objects, and the upper-limits are the $3\,\sigma$ of the bootstrap resampling.

4 Dust obscuration

Relation $L_{\rm FUV}$ - $L_{\rm IR}/L_{\rm FUV}$. Figure 3 left-up shows our measurements of the ratio of IR to UV luminosity (IRX) as a function of UV luminosity. We are in agreement with [12] using UV-selected galaxies. We find that there is no evolution in the ratio of IR to UV luminosity as a function of UV luminosity for the mean population.

Relation M_* - $L_{\rm IR}/L_{\rm FUV}$. The stellar mass has been shown to correlate with the dust attenuation in LBGs [22] and UV-selected galaxies [12]. [22] suggested that the metallicity has an important correlation with the stellar mass, UV-slope and IRX for LBGs at $z \sim 2$, which is increasing with them. Those relation tell us that the massive galaxies have a larger dust attenuation due to the metallicity abundance. The results from [12] suggest that there is no significant evolution with the redshift of the dust attenuation at a given stellar mass for UV-selected galaxies. Figure 3 right-up shows our measurements of the ratio of IR to UV luminosity as a function of stellar mass. Also, we obtain a good agreement with the UV-selected galaxies [12].

Relation $\beta_{\rm UV}$ - $L_{\rm IR}/L_{\rm FUV}$. Previous works have shown that the local starburst relation by [18] (M99, 1999) is valid for LBGs at various redshifts: [14, 15] found that the UV star-formation rates of LBGs stacked at $z \sim 3$ corrected by attenuation obtain using M99 relation presents a good match with the far-IR and radio estimates. However, [20] found that the ratio of IR to UV luminosity for the LBGs detected in PACS at $z \sim 3$, extremely dusty and no representative of all LBGs sample, is much higher that predicted by the M99 relation. Figure 3 down shows our measurements of the ratio of IR to UV luminosity as a function of beta. The curves for local starburst galaxies from M99 and the correction by [26], T12, to M99 law are plotted. We also present the LBGs detected in PACS by [20] at $z \sim 3$. It can be seen that our results are between the M99 and T12 relations. Also, they are in agreement with the results for individual lens LBGs (cB58 and cosmos eye, [24]). [4] showed that the galaxies up to $z \sim 4$ are located between M99 and T12.

5 Main sequence

The "main sequence" of star-forming galaxies is the term coined to describe the relatively tight correlation between SFR and stellar mass, and the relation is known to evolve with redshift and increase with stellar mass. In Fig. 4 we show the location of our stacked points in the (SFR vs M_*) diagramm, they do follow a sequence that might be interpreted as an evolution of the SFR vs M_*.

6 Conclusions

We perform a stacking analysis on a large sample of LBGs ($\sim$22 000) to study their dust properties. We obtain the full infrared spectral energy distributions of our LBGs as a function of their ultraviolet luminosity $L_{\rm UV}$, their UV slope $\beta_{\rm UV}$ and their stellar mass M_* and we can characterize them in terms of their dust attenuation and SFR. A full description of this

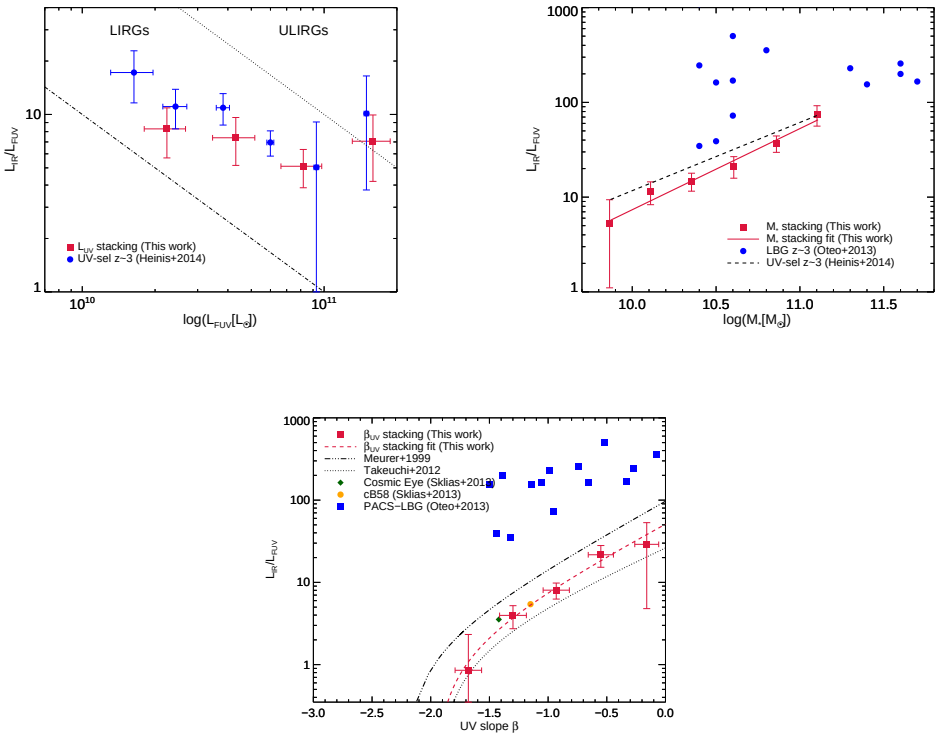

Figure 3: Dust attenuation obtained using the stacking as a function of $L_{\rm FUV}$ (left-up), stellar mass (right-up) and UV slope (down).

work will be submitted to A&A soon (Álvarez-Márquez et al., in prep.)

References

[1] Aretxaga et al. (2011), MNRA, 415, 4

[2] Bavouzet (2008), PhD thesis, Université du Paris sud XI

[3] Béthermin et al. (2010), A&A, 516, A43

[4] Burgarela et al. (2013), A&A, 554,A70

[5] Burgarella et al. (2005), MNRAS, 360, 1411)

[6] Capak et al. (2007), ApJS, 172, 99

[7] Coppin et al. (2014), arXiv:1407.6712

[8] Daddi et al. (2007), ApJ, 670, 157

[9] Dale et al. (2014), ApJ, 784, 83

[10] Dole et al. (2006), A&A, 451, 417

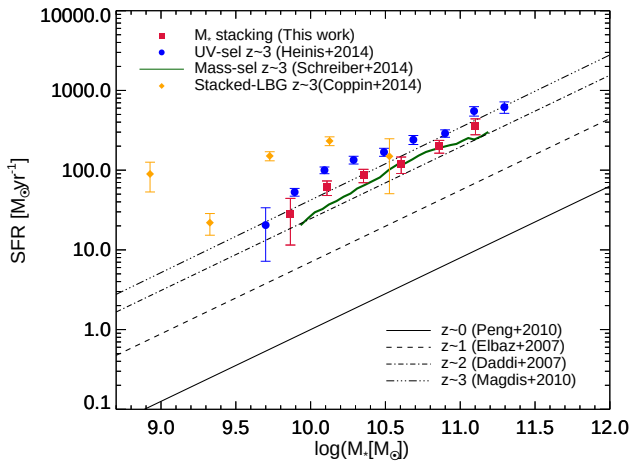

Figure 4: All of the points correlations shown take into account the total (unobscured + obscured) SFR versus stellar mass. The observed correlations are plotted at $z = 0$ [21], $z = 1$ [11], $z = 2$ [8] and $z = 3$ ([14], based of IRAC detected LBGs). The red square are our measurements, and the have a good agreement with previous works for UV-selected galaxies (Blue dots, [12]), for Mass-complete sample for star-forming galaxies (green line, [23]) and the LBGs sample (yellow diamonds, [7]).

[11] Elbaz et al. (2007), A&A, 468, 33

[12] Heinis et al. (2014), MNRA, 437, 1268

[13] Lutz et al. (2011), A&A, 532, A90

[14] Magdis et al. (2010a), MNRA, 401, 1521

[15] Magdis et al. (2010b), ApJ, 714, 1740

[16] McCracken et al. (2012), A&A, 544, A156

[17] Noll et al. (2009), A&A, 507, 1793

[18] Meurer, Heckman & Calzetti (1999), ApJ, 521, 64

[19] Oliver et al. (2011), MNRA, 424, 1614

[20] Oteo et al. (2013), A&A, 553, L3

[21] Peng, Y.-j., Lilly, S. J., Kovač, K., et al. 2010, ApJ, 721, 193

[22] Reddy et al. (2010), ApJ, 712, 1070

[23] Schreiber et al. (2014), arXiv:1409.5433

[24] Sklias et al. (2014), A&A, 561, 149

[25] Steidel et al. (1996), ApJ, 462, L17

[26] Takeuchi et al. (2012), ApJ, 755, 144